Supplementary Material for "Thermal Management of Air-Cooling Lithium-Ion Battery Pack"

Conversation equations

The partial differential equations (PDEs) are employed to describe the conservation of charge and mass in solid and liquid phases. In the pseudo-two-dimensional model, the active electrode material is considered to be composed of uniform spherical particles with the same size.

Fick's second law is used to describe the diffusion of lithium ions in particles.

$$\frac{\partial c_{s,i}}{\partial t} = \frac{D_{s,i}}{r^2}\frac{\partial}{\partial r}\left(r^2 \frac{\partial c_{s,i}}{\partial r}\right) \tag{1}$$

where $i = n \,\&\, p$, n is the negative electrode, p is the positive electrode, $c_{s,i}$ is the lithium-ion concentration in the solid phases, $D_{s,i}$ is the lithium-ion diffusion coefficient in the solid phases. The boundary conditions are as follows,

$$\left.\frac{\partial c_{s,i}}{\partial r}\right|_{r=0} = 0, D_{s,i}\left.\frac{\partial c_{s,i}}{\partial r}\right|_{r=R_{s,i}} = -\frac{J_i}{a_{v,i}F} \tag{2}$$

where $R_{s,i}$ is the radius of spherical material particles, J_i is the local current density, and $a_{v,i}$ is the specific surface area of spherical material particles.

Based on the concentrated solution theory, the concentration of lithium ion in the liquid phase of porous electrode can be described by the following equation,

$$\varepsilon_{e,i}\frac{\partial c_e}{\partial t} = \frac{\partial}{\partial x}\left(D_{e,i}^{eff}\frac{\partial c_e}{\partial x}\right) + a_{v,i}t_0^+\frac{J_i}{F} \tag{3}$$

where $\varepsilon_{e,i}$ is the volume fraction of liquid phase, $D_{e,i}^{eff}$ is the effective diffusion coefficient of lithium ion in liquid phase, and t_0^+ is the lithium ion migration number. The boundary condition is,

$$\begin{cases} \left.D_{e,i}^{eff}\frac{\partial c_e}{\partial x}\right|_{x=0} = 0, \left.D_{e,i}^{eff}\frac{\partial c_e}{\partial x}\right|_{x=L} = 0 \\ \left.D_{e,i}^{eff}\frac{\partial c_e}{\partial x}\right|_{x=(\delta_-)^-} = \left.D_{e,i}^{eff}\frac{\partial c_e}{\partial x}\right|_{x=(\delta_-)^+}, \left.D_{e,i}^{eff}\frac{\partial c_e}{\partial x}\right|_{x=(\delta_- + \delta_{sep})^-} = \left.D_{e,i}^{eff}\frac{\partial c_e}{\partial x}\right|_{x=(\delta_- + \delta_{sep})^+} \\ \left.c_e\right|_{x=(\delta_-)^-} = \left.c_e\right|_{x=(\delta_-)^+}, \left.c_e\right|_{x=(\delta_- + \delta_{sep})^-} = \left.c_e\right|_{x=(\delta_- + \delta_{sep})^+} \end{cases} \tag{4}$$

The charge conservation in porous electrode is described by Ohm's law,

$$\sigma_i^{eff}\frac{\partial \varphi_{s,i}}{\partial x} = J_i \tag{5}$$

where σ_i^{eff} is the effective conductivity in the solid phase and $\varphi_{s,i}$ is the potential

in solid phase. Here we consider that the negative electrode is electrically grounded, and the boundary condition is,

$$\varphi_s\big|_{x=0} = 0\ \mathrm{V}, -\sigma_n^{eff}\left.\frac{\partial \varphi_s}{\partial x}\right|_{x=\delta_-} = -\sigma_i^{eff}\left.\frac{\partial \varphi_s}{\partial x}\right|_{x=\delta_-+\delta_{sep}} = 0, -\sigma_i^{eff}\left.\frac{\partial \varphi_s}{\partial x}\right|_{x=\delta_-+\delta_{sep}+\delta_+} = \frac{I_{app}}{A} \quad (6)$$

where I_{app} is the applied current.

The charge conservation in the liquid phase of the porous electrode is described by the following equation,

$$\kappa_i^{eff}\frac{\partial \varphi_e}{\partial x} = -J_i + \kappa_i^{eff}\frac{2RT}{F}\left(1-t_0^+\right)\left[1+\frac{\partial \ln f}{\partial \ln\left(\frac{c_e}{c^\Theta}\right)}\right]\frac{\partial \ln\left(\frac{c_e}{c^\Theta}\right)}{\partial x} \quad (7)$$

where κ_i^{eff} is the lithium-ion effective conductivity in liquid phase, f is the activity coefficient, c^Θ is the standard concentration, $c^\Theta = 1\ \mathrm{mol\cdot m^{-3}}$. The boundary condition is,

$$\begin{cases} \left.\frac{\partial \varphi_{e,i}}{\partial x}\right|_{x=0} = \left.\frac{\partial \varphi_{e,i}}{\partial x}\right|_{x=\delta_-+\delta_{sep}+\delta_+} = 0 \\ -\kappa_i^{eff}\left.\frac{\partial \varphi_e}{\partial x}\right|_{x=(\delta_-)^+} = -\kappa_i^{eff}\left.\frac{\partial \varphi_e}{\partial x}\right|_{x=(\delta_-)^-}, -\kappa_i^{eff}\left.\frac{\partial \varphi_e}{\partial x}\right|_{x=(\delta_-+\delta_{sep})^+} = -\kappa_i^{eff}\left.\frac{\partial \varphi_e}{\partial x}\right|_{x=(\delta_-+\delta_{sep})^-} \end{cases} \quad (8)$$

The liquid concentration in the separator is described by the following equation,

$$\varepsilon_{e,sep}\frac{\partial c_e}{\partial t} = \frac{\partial}{\partial x}\left(D_{e,sep}^{eff}\frac{\partial c_e}{\partial x}\right) \quad (9)$$

where $\varepsilon_{e,sep}$ is the volume fraction of liquid phase, and $D_{e,sep}^{eff}$ is the effective diffusion coefficient of lithium ion in the liquid phase in the separator. The boundary condition is,

$$\left.\frac{\partial c_e}{\partial x}\right|_{x=\delta_+} = \left.\frac{\partial c_e}{\partial x}\right|_{x=\delta_++\delta_{sep}} = 0 \quad (10)$$

The potential in the separator is described by the following equation,

$$\kappa_{sep}^{eff}\frac{\partial \varphi_e}{\partial x} = -\frac{I_{app}}{A} + \kappa_{sep}^{eff}\frac{2RT}{F}\left(1-t_0^+\right)\left[1+\frac{\partial \ln f}{\partial \ln\left(\frac{c_e}{c^\Theta}\right)}\right]\frac{\partial \ln\left(\frac{c_e}{c^\Theta}\right)}{\partial x} \quad (11)$$

where A is the area of the electrode plate and κ_{sep}^{eff} is the effective conductivity of the liquid phase in the separator. The boundary conditions are as follows,

$$\left.\frac{\partial \varphi_e}{\partial x}\right|_{x=\delta_+} = \left.\frac{\partial \varphi_e}{\partial x}\right|_{x=\delta_+ +\delta_{sep}} = 0 \tag{12}$$

In addition, there are some additional equations to describe some of the above physical quantities,

$$\begin{cases} a_{v,i} = \dfrac{3\varepsilon_{s,i}}{R_{s,i}}, i = n, p \\ D_{e,i}^{eff} = D_{e,i}\varepsilon_{e,i}^{1.5}, i = n, sep, p \\ \sigma_i^{eff} = \sigma_i \varepsilon_{s,i}^{1.5}, i = n, p \\ \kappa_i^{eff} = \kappa_i \varepsilon_{e,i}^{1.5}, i = n, sep, p \end{cases} \tag{13}$$

where $D_{e,i}$ is the lithium-ion diffusion coefficient in liquid phase, σ_i is the solid conductivity and κ_i is the liquid conductivity.

Butler-Volmer equation are used to describe the relationship between the local current density at the solid-liquid interface and the overpotential of intercalation/deintercalation reaction,

$$J = i_0 \left[\exp\left(\frac{\alpha_a F}{RT} \eta \right) - \exp\left(\frac{-\alpha_c F}{RT} \eta \right) \right] \tag{14}$$

where i_0 is the exchange current density, which is determined by the concentration of lithium ion in the liquid phase and the concentration of lithium ion at the solid-liquid interface, $i_0 = k_a \left(\mathrm{c}_{s,\max} - \mathrm{c}_{s,surf} \right)^{\alpha_c} c_{s,surf}^{\alpha_a} c_e^{\alpha_a}$, where k_a is the rate constant of intercalation/deintercalation reaction, α_a and α_c is the anode transfer coefficient and the cathode transfer coefficient, respectively. η is the overpotential which is related to solid phase potential, liquid phase potential and equilibrium potential, $\eta = \varphi_s - \varphi_e - E_{eq}$.

Physical properties

Table 1 presents the geometric parameters required for pseudo-two-dimensional model and the physical quantities required for numerical simulation. Table 2 presents the geometric parameters required for single battery model and the battery pack model.

Table 1. Parameter of the pseudo-two-dimensional model

Parameter	Value	Parameter	Value
Length of negative electrode (δ_{neg})	5.5×10^{-5} m	Charging cutoff voltage ($E_{\max}$)	4.1 V
Length of separator (δ_{sep})	3×10^{-5} m	Discharging cutoff voltage ($E_{\min}$)	2.5 V
Length of positive electrode (δ_{pos})	4×10^{-5} m	Initial lithium ion concentration in electrolyte ($c_{e,0}$)	1200 mol/m^3
Particle radius of positive electrode material (r_{pos})	2.5×10^{-7} m	Volume fraction of material in positive electrode ($\varepsilon_{s,pos}$)	0.42
Initial lithium-ion concentration in positive electrode ($c_{pos,\max}$)	48000 mol/m^3	Volume fraction of other filling in positive electrode ($\varepsilon_{f,pos}$)	0.17
Concentration of chloride ion in the electrolyte ($c_{cl,e}$)	1200 mol/m^3	Volume fraction of electrolyte in positive electrode ($\varepsilon_{e,pos}$)	0.41
Exchange current density in positive electrode ($I_{0,pos}$)	36.61 A/m^2	Exchange current density in negative electrode ($I_{0,neg}$)	0.96 A/m^2

Table 2. Parameter of the battery pack model

Parameter	Value	Parameter	Value
Battery radius (r_{batt})	9 mm	Inlet temperature (T_{inlet})	298.15 K
Battery height (h_{batt})	65 mm	Initial temperature (T_{init})	298.15 K
Mandrel radius ($r_{mandrel}$)	2 mm	Connector radius ($r_{connector}$)	0.003 m
Battery thermal conductivity, angular ($k_{T,batt,ang}$)	32.512 W/(m ·K)	Connector height ($h_{connector}$)	0.003 m
Battery thermal conductivity, radial ($k_{T,batt,r}$)	0.85807 W/(m ·K)	Air velocity at the entrance	3.159×10^{-6} m^3/s
Battery density (ρ_{batt})	2026.4 kg/m ^{3}	Battery heat capacity ($C_{p,batt}$)	1412.8 J/(kg ·K)

Numerical model validation

The voltage of the battery obtained from the simulation model is compared with the result in the literature, in order to demonstrate the reliability of our model[1]. The voltage rise rate gradually decreases as charging as shown in Fig. S1. The maximum error of the voltage between the experiment and simulation results does not exceed 0.2 V. It proves that our mathematical model is reasonable.

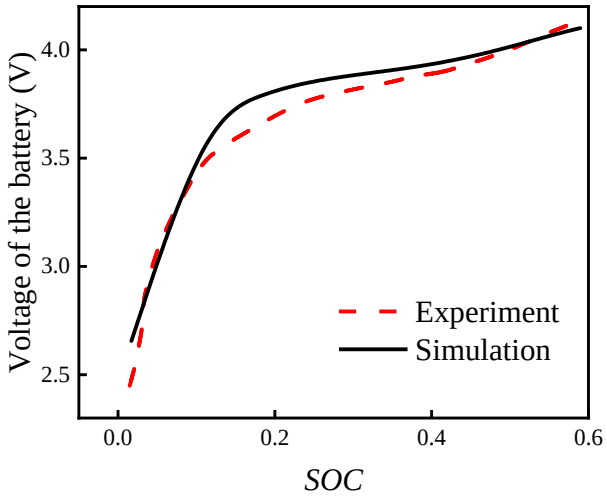

Figure S1. The voltage of the battery obtained by experiment and simulation

Thermal analysis of battery pack without forced air cooling

Fig. S2 shows the temperature distribution in the battery pack at the end of a single charge-discharge cycle without air cooling. The result shows that the temperature in the pack is high and the temperature distribution is uniform. During the charging process, each battery is considered as a heat source. In addition to the heat generated by the battery itself, the heat generated by the surrounding batteries will also cause the temperature of the battery to rise. The highest temperature of the pack is 325 K, which is not the proper operating temperature. Therefore, the forced air-cooling system is applied into the battery pack for the operational stability and safety.

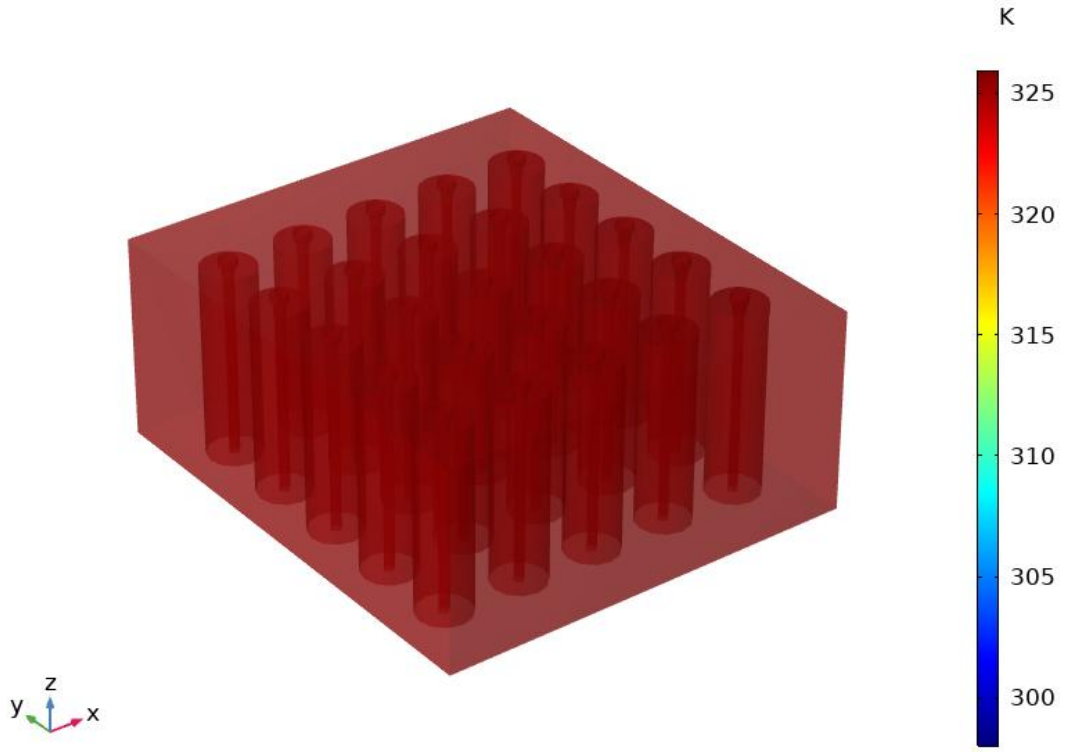

Figure S2. The temperature distribution of the battery pack without air-cooling system

Fig. S3 and Fig. S4 show the time-dependent temperature in different battery pack using stagger arrangement and trapezoid arrangement. For the staggered arrangement and trapezoidal arrangement, the ventilation strategy with air inlet above and outlet below is the best. As shown in Fig. S3 and Fig. S4, the batteries in the battery packs have low temperatures and uniform temperature distribution when the air-cooling device is on the top and the air outlet on the bottom.

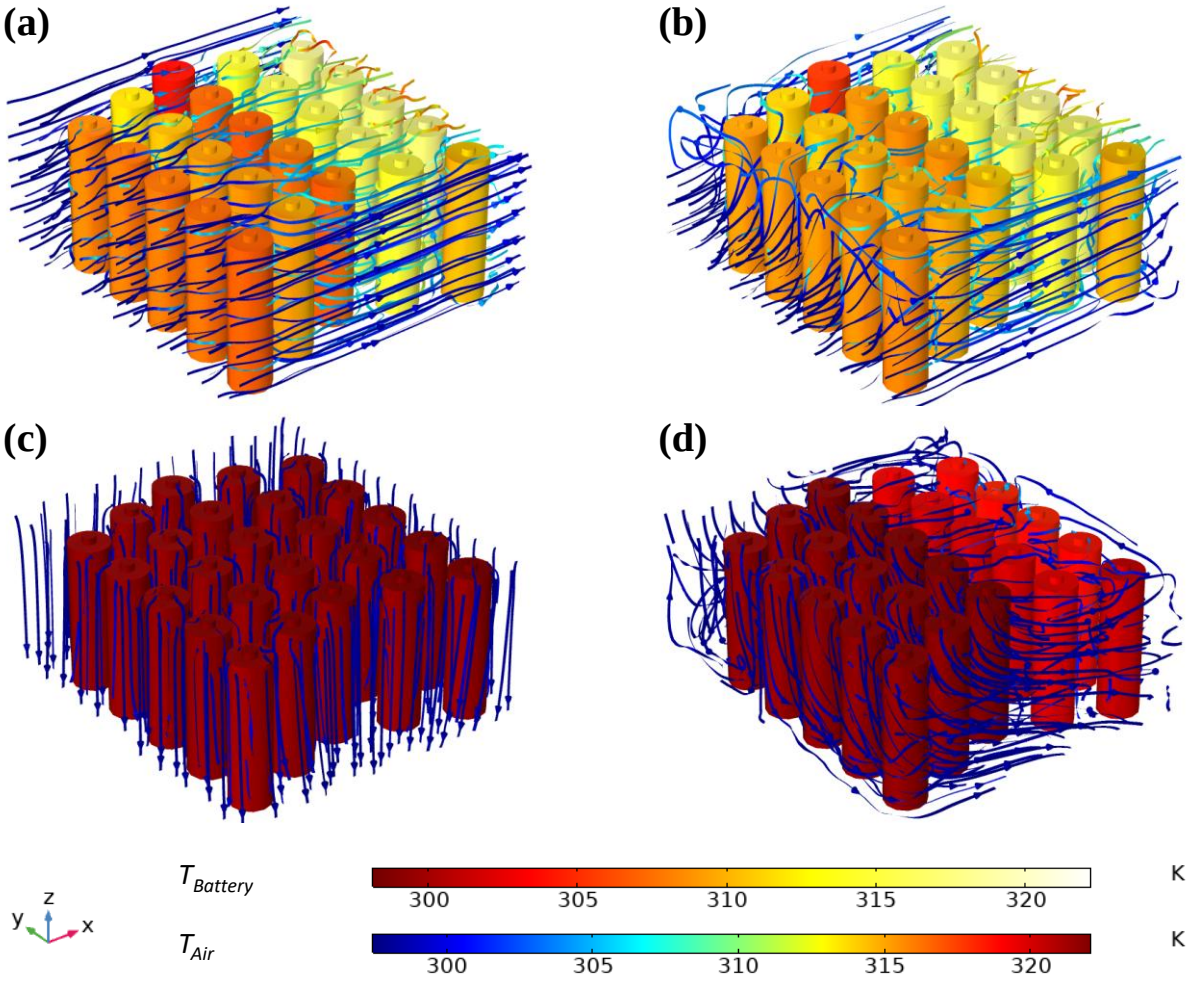

Figure S3. Temperature distribution of the battery packs with different inlet and outlet positions for stagger arrangement. (a) The air inlet is on the left and the outlet is on the right. (b) The air inlet is on the lower left side and the outlet is on the upper right side. (c) The air inlet is on the upper side and the outlet is on the lower side. (d) The air inlet is on the upper left and the outlet is on the lower right.

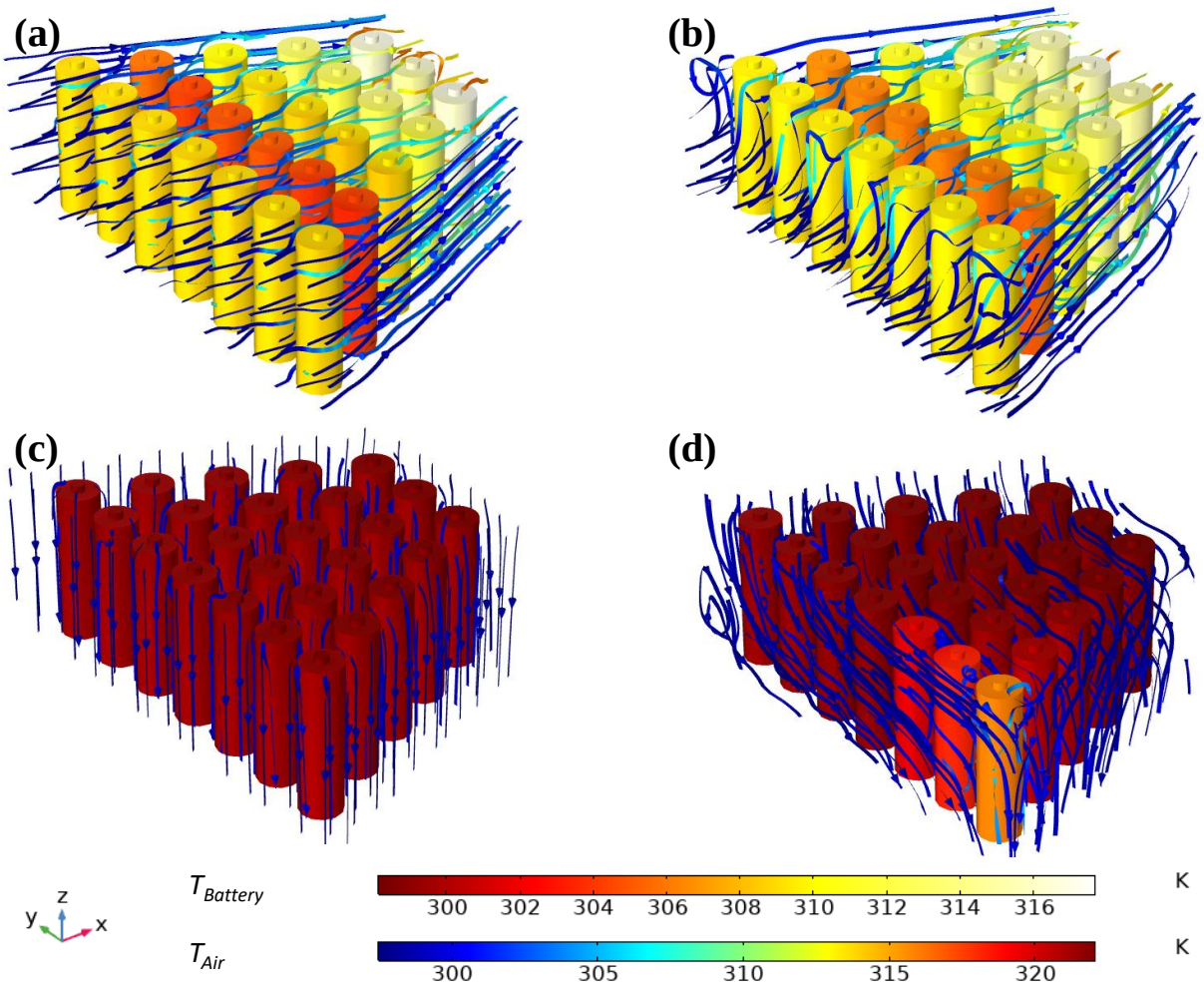

Figure S4. Temperature distribution of the battery packs with different inlet and outlet positions for trapezoid arrangement. (a) The air inlet is on the left and the outlet is on the right. (b) The air inlet is on the lower left side and the outlet is on the upper right side. (c) The air inlet is on the upper side and the outlet is on the lower side. (d) The air inlet is on the upper left and the outlet is on the lower right.

1. Yudha, C. S.; Muzayanha, S. U.; Widiyandari, H.; Iskandar, F.; Sutopo, W.; Purwanto, A., Synthesis of LiNi0.85Co0.14Al0.01O2 Cathode Material and its Performance in an NCA/Graphite Full-Battery. *Energies* **2019,** *12* (10), 1886.